Using a new HSPC aging model in vitro to explore the mechanism of cellular memory in aging HSPCs

Yongpin Dong
Changzheng Hospital
Wenfang Li
Changzheng Hospital
Wuxiong Zhou
Shanghai University of Traditional Chinese Medicine
Lina Zhang (zln_1250@163.com)
Shanghai University of Traditional Chinese Medicine https://orcid.org/0000-0001-5804-2252

Research Article

Keywords: Aging model, HSPC, cellular memory, TOPOIIα, UHRF1

Posted Date: February 25th, 2021

DOI: https://doi.org/10.21203/rs.3.rs-238429/v1

Version of Record: A version of this preprint was published at Stem Cell Research & Therapy on August 9th, 2021. See the published version at https://doi.org/10.1186/s13287-021-02455-x.

Abstract

Age-associated changes attenuate human blood system functionality through the aging of hematopoietic stem and progenitor cells (HSPCs). Hematopoietic aging is manifested in human populations in the form of an increase in myeloproliferative disease,therefore, study on hematopoietic stem and progenitor cells (HSPCs) senescence bears great significance to treat hematopoietic associated disease. However, the mechanism of HSPC aging is lacking, especially cellular memory mechanism. Here, we not only reported a new HSPC aging model in vitro, but also propose and verify the cellular memory mechanism of HSPC aging of Polycomb/Trithorax system. In this model cells, the senescence-related β-gal activity, cell cycle, colony-forming ability, aging-related cell morphology and metabolic pathway are significantly changed compare to the young group. Furthermore, we found the model HSPCs have more obvious aging manifestation than those of natural mice and IL3 is the major factor contributing to HSPC aging in the model. We also observed dramatically changes in the expression level of PRC/TrxG complexes. We further identified downstream molecules of PRC/TrxG complexes,Uhrf1 and TopII, which were found to play a critical role in HSPC aging based on the HSPC aging model. So, these findings proposed a new aging HSPC model in vitro which we forecasted could be used to preliminary screen the drugs of the HSPC aging related hemopathy and suggested cellular memory mechanism of HSPC aging.

Introduction

The mammalian blood system is a highly differentiated and dynamic, most blood cells are the mostly short-lived and quickly replaced within few days.It is established that most of mature blood cells are constantly generated and replaced from hematopoietic stem cells (HSCs) through a series of lineage-committed hematopoietic progenitor cells (HPCs)[1], so mammals maintain hematopoiesis by the activity of thousands of hematopoietic stem and progenitor cells (HSPCs)[1-4]. Although the blood is the definitive self-renewing tissue of the body, it does not escape the aging process. The previous study indicated age-related alterations in the human blood system depends on hematopoietic stem and progenitor cells (HSPCs) aging[5-7]. Hematopoietic aging is manifested in human populations in the form of an increase in myeloproliferative disease, including leukemias, declining adaptive immunity , and greater propensity to anemia.Therefore, study on hematopoietic stem and progenitor cells (HSPCs) senescence bears great significance to treat hematopoietic associated disease. Furthermore, stem cells are exposed to both intrinsic and extrinsic assault over their lifetime,thus, it has been hypothesized that aging or functional failure of stem cells may limit tissue repair and renewal, thereby contributing to overall organismal aging and life span reduction [8].Therefore, besides great significance to treat hematopoietic disease, study on HSC /HSPC senescence also bears great significance to further elucidate the mechanisms of aging.

Aging hematopoietic stem and progenitor cells model in vitro is an important platform to study HSC/HPC senescence and associated diseases [9]. To date, here were some ways to build aging HSC/HSPC models in vitro including old animal model[10], busulfan induced cell aging model[11], radiation-induced cell aging model[12] and t-BHP induced cell aging model[13]. However, these ways were limited either by long

experimental periods or complicated operation steps. Our study proposed a quick and easy method of obtaining aging HSPC in vitro.

Compared with the other aging theories, the mechanism of HSC/HSPC aging remains less known. Besides the known players such as DNA damage, telomere shortening and oxidative stress, cellular memory maybe very important in HSC aging process[14-15]. During development of multicellular organisms, cells become different from one another by distinct use of their genetic program in response to transient stimuli, an example being lineage specification in hematopoiesis[16]. Long after such a stimulus has disappeared, cellular memory mechanisms still enable cells to “remember” their chosen fate over many cell divisions. Cellular memory is a dynamic balance between the Polycomb (PcG) and Trithorax (TrxG) group proteins, then their target genes[14, 17-19]. PcG and TrxG group proteins are essential epigenetic regulators that can maintain stable epigenetic memory of silent states (via PcG) and active states (via TrxG) of their target genes. However, the mechanism of cellular memory including PcG/TrxG sysytem alteration that occurs in HSPC aging process remains less known. Our previous study demonstrated that the gene expression of PcG and TrxG proteins was significantly altered in HSPCs($Lin^-c\text{-}kit^+$) of old mice[18]. In the present study, based on our new HSPC aging model, we further explored PcG/Trx G proteins expression alteration and the histone methylation regulatory on their target genes TOPOIIα and UHRF1.

Materials And Methods

Animals and major regents

Equal numbers of male and female C57BL/6J SPF mice were obtained from Shanghai Sippr-BK Experimental Animal Center [Certificate No. SCXK (Shanghai) 2013- 0016]. Young mice were 4 weeks of age and 16-18 g in weight, old mice were 18 months of age and 25-30 g in weight.

Reagents

Red blood cell lysis buffer, SA-β-Gal staining kit and cell cycle detection kit were purchased from Beyotime Biotechnology Co.; Lineage Cell Depletion kit and Anti-c-kit(CD117) MicroBead kit were purchased from Miltenyi Biotec Co.; TUNEL Apoptosis Detection Kit (Alexa Fluor 647) was purchased from Shanghai Yeasen Biotechnology Co.; RNA Extraction and Purification kit, Reverse Transcription and Fluorescence Quantitative PCR kit were purchased from Takara Co.. Stemspan Stem Cell Media, Mouse Colony- Forming Unit (CFU) Assays Using MethoCult™ were purchased from Stem cell Co.; mouse SCF, mouse IL-3 and mouse IL-6 were purchased from Novus Biologicals Co.; anti-H3K4me3, anti-H3K27me3, anti-MLL1, anti-Trx, anti-Ezh2 and anti-BMI1 were purchased from CST Co.; anti-Mel18 was purchased from Abcam Co.; lipofectamine 3000 was purchased from Invitrogen Co.; Opti-MEM was purchased from GIBCO Co. .

Isolation and purification of HSPCs

Mice were sacrificed by cervical dislocation. The femur was elevated and bone marrow was rinsed. The filtrate was centrifuged and the pellet was suspended in red blood cell lysis buffer, centrifuged at 3000 rpm, 5 min. The precipitate was bone marrow mononuclear cells (MNCs)(Fig.1a). MNCs were suspended in PBS containing EDTA and 0.5% BSA. Then we got HSPC by using $Lin^{-}c\text{-}kit^{+}$ immunomagnetic beads sorting technique with lineage cell depletion kits and anti-c-Kit microbeads(Fig.1b). All the animal experiments were performed in compliance with the guidelines of the Animal Care and Use Committee of SHUTCM.

Flow Cytometry Analysis

Cellular purity was detected with flow cytometer before and after sorting: to test HSPCs purity, 10^6 MNCs (unpurified) and 10^6 $Lin^{-}c\text{-}kit^{+}$ MNCs(purified) were collected. 10ul CD117-PE was added to the cells. The cells were resuspended in FACS buffer, and analyzed by flow cytometry using a Becton Dickinson Accuri™ C6.

The establishment and identification of Old HSPCs model

1)Young group: HSPCs were isolated from 4- weeks-old mouse according to the steps above;

2) aging Model group : Young HSPCs were cultured with the modeling medium (Stemspan Stem Cell Media + 10 ng/ml IL3 + 10 ng/ml IL6 + 30 ng/ml SCF) for 8 days(Fig.1c). The modeling medium was changed every 2 to 3 days;

3)old mouse group: HSPCs were isolated from 18-months-old mouse according to the steps above.

SA-β-gal staining

HSPCs(～1000,000 cells) were collected on day2,4,6,8, respectively. They were all fixed with 4% paraformaldehyde for 15 minutes. The cells were incubated at 37ºC without CO_2 for 16 h in β-galactosidase staining solution. The number of β-galactosidase positive cells per 400 total cells was counted.

Cell cycle

HSPCs(～1000,000 cells) were collected, fixed with cold 4% paraformaldehyde for 1h and fixed with 70% ethanol overnight at 4℃. Cells were then incubated in propidium iodide staining solution (Beyotime) for 30 min at 37℃ in the dark. The cell cycle distribution was analyzed by flow cytometry with FACS Express software.

Mixed colony-forming unit (CFU-Mix) of HSPC culture

Cells(～1000,00cells) were collected and subjected to CFU culture: Cells were diluted, in duplicate, with IMDM+2% FBS and MethoCult™ GF M3434 medium to a final concentration of 5×10^3 per 35mm dish. 0.3 mL of the diluted cells were added to 3mL of MethoCult™ and mixed thoroughly. The final cell mixture was dispensed into each 35 mm dish at a volume of 1.1 mL and incubated at 37ºC in 5% CO_2 for 7 days. Photos were taken using an inverted microscope. Finally, we added 1mg/ml p-iodonitrotetrazolium violet to 24-well cells so as to take photos 24 hours later. The number of CFU-Mix per 5×10^3 cells represented the pluripotency of the HSPCs.

Transmission Electron Microscope (TEM)

Cells(～1000,000 cells) were prefixed with 2.5% glutaraldehyde and then dehydrated with an ethanol gradient series before being embedded in Epon812. Samples were cut into 50-70nm thick sections by a microtome. All samples were observed under a transmission electron microscope (TEM) (JEM- 2100, JEOL, Japan).

Isobaric tags for relative and absolute quantification (iTRAQ)

Protein digestion and iTRAQ labeling were performed as described previously[20]. Briefly, 100 ug of protein from each sample was reduced, alkylated then digested with sequence-grade modified trypsin (Promega, Madison, WI) prior to labeling with one of the individual 8-plex-iTRAQ tags (Applied Biosystems, Framingham, MA). The peptide mixture was fractionated by high pH separation using Ultimate 3000 system (Thermo Fisher scientific, MA, USA) connected to a reverse phase column (XBridge C18 column, 4.6mm x 250 mm, 5μm, Waters Corporation, MA, USA). Twelve fractions were separated by nanoLC and analyzed by on-line electrospray tandem mass spectrometry. The experiments were performed on an Easy-nLC 1000 system (Thermo Fisher Scientific, MA, USA) connected to a Q-Exactive mass spectrometer (Thermo Fisher Scientific, MA, USA) equipped with an online nano-electrospray ion source. PEAKS DB was set up to search the Uniprot-mouse database (ver.201711, 51946 entries) assuming the digestion enzyme Trypsin. Differently expressed proteins were filtered if their fold changes were over 1.5 and contained at least 2 unique peptides with P (PEAKSQ) below 0.01.

RNA-seq, Library Generation, and Bioinformatics Analysis.

HSPCs(～1000,000 cells) were collected. Total RNA was isolated using RNeasy mini kit (Qiagen, Germany). Strand-specific libraries were prepared using the TruSeq® Stranded Total RNA Sample Preparation kit (Illumina, USA). Briefly, mRNA was enriched with oligo(dT) beads. Following purification, the mRNA is fragmented into small pieces using divalent cations under 94°Cfor 8 min. The cleaved RNA fragments are copied into first strand cDNA using reverse transcriptase and random primers. This is

followed by second strand cDNA synthesis using DNA PolymeraseI and RNaseH. These cDNA fragments then go through an end repair process, the addition of a single ‘A’ base, and then ligation of the adapters. The products are then purified and enriched with PCR to create the final cDNA library. Purified libraries were quantified by Qubit® 2.0 Fluorometer (Life Technologies, USA) and validated by Agilent 2100 bioanalyzer (Agilent Technologies, USA) to confirm the insert size and calculate the mole concentration. Cluster was generated by cBot with the library diluted to 10pM and then were sequenced on the Illumina HiSeq X ten (Illumina, USA). The library construction and sequencing was performed at Shanghai Biotechnology Corporation, Shanghai, China. For GO enrichment analysis, selected differentially regulated genes between young group and old group HSPCs with a Fisher-test-corrected $P < 0.05$ were analyzed on the Gene Ontology Consortium website (geneontology.org). Like GO enrichment, association of the genes with different path-ways was computed with the Kyoto Encyclopedia of Genes and Genomes (KEGG) (http://www.genome.jp/kegg) databases. All data are representative of three independent experiments.

TrxG/PcG disequilibrium

Quantitative RT-PCR

Quantitative real-time polymerase chain reaction(qRT-PCR) was used to verify the gene expression of PCG proteins(EZH1, BMI-2, EED, MEL18, Rae-28) and TRXG proteins(MLL, Trx). Total RNA extraction and reverse transcription were performed according to the manufacturer’s instructions of the kits(9108/9109,Takara; RR047A, Takara). The A260/280 ratio of RNA was detected.The primers were designed and synthesized by sango biotech. The β-actin (internal control) primers were used. All primer sequences are listed.β-actin (internal control): 5'-AACGCAGCTCAGTAACA GT CC-3'(forward);β-actin (internal control): 5'-GTACCACCATGTACCCAGGC-3'(reverse); Ezh2: 5'-AGCAGTAAGAGCAGCAGCAA-3' (forward); Ezh2: 5'-TTCCTTCCATGC AA CACCCA-3'(reverse); Bmi-1: 5'-GGACTGGGCAAACAGGAAGA-3' (forward); Bmi-1: 5'-GACTCTGGGAGTGACAAGGC-3'(reverse); Eed: 5'-GCTCAGCCTGATCGAATG CT-3' (forward); Eed: 5'-TTGGCGATGGGATCGACTTC-3'(reverse); Mel18: 5'-TCCCC ATCTCCATTCTCCGT-3' (forward); Mel18: 5'-ATACCCCCTGACAGAGGTCC-3' (reverse); Rae-28: 5'-GCACAGATCTTGAGAGCAGG-3' (forward); Rae-28: 5'-GCAA GGCTGCCAAGAGATTG-3'(reverse); Trx: 5'-TAAAGCAGTGGCTTAGGGGAC-3' (forward); Trx: 5'-GAGAGTCTATACCCAACTGCCA-3'(reverse); Mll: 5'-ACGCT TG TCTGTCTGGATGG-3' (forward); Mll: 5'-CCCATGAGATTCCGGCACTT-3'(reverse).

SYBR green dye was used for Real-time quantitative PCR (RR420A, Takara). The $2^{-\Delta Ct}$ method was used to calculate mRNA expression levels. $\Delta Ct=Ct_{target\ gene} - Ct_{internal\ control\ gene}$ (where Ct is the cycle number when the fluorescence signal reaches the set threshold). The amplification parameters were: 95ºC for 30 s, (95ºC for 5 s, 60ºC for 34 s) for 40 cycles.The analysis was performed with three biological replicates.

Western Blot

Cells were lysed with RIPA lysis containing protease inhibitor. Cell lysates were collected and the total protein content was estimated by the Bradford method (Bio-Rad).An aliquot of 70 µg of protein extract was loaded in each lane and separated in a 10% SDS-PAGE gel and electroblotted on a PVDF membrane.Membrane was then blocked with 4% BSA in 1× TBS and 0.1% TWEEN®20, washed and probed using antibodies directed against EZH1(enhancer of zeste homolog 1), BMI-2 (B lymphoma mo-MLV insertion region 2), EED (embryonic ectoderm development), MLL (mixed lineage leukemia), MEL18 (melanoma nuclear protein 18), Rae-28 (polyhomeotic-like protein 1), TOPOIIα(DNA topoisomerase 2-alpha), UHRF1 (ubiquitin-like with PHD and ring finger domains 1), H3K27me3, H3K4me3 and GAPDH (endogenous loading control) overnight at room temperature. Blots were then washed and incubated with (i) 1:2000 dilution of HRP secondary antibody for 2 h at room temperature. The protein bands were developed with the chemiluminescent reagents (Millipore). Relative band intensities were determined by using ImageJ software.

Small interfering RNA (siRNA)

Based on significant down-regulation of Bmi-2 and Trx in the model group, Bmi-2 and Trx were selected for Small interfering RNA to validate their effect on the target gene UHRF1 and TOPO and aging-related manifestations. Three siRNAs targeting Bmi-2 and Trx were designed and synthesized, respectively. Transfection: Cells were collected and resuspended in HSPCs medium without cytokines. 20 pM of siRNA was added to 50µl of Opti-MEM serum-free medium; an equivalent amount of irrelevant siRNA was added as a negative control. Mixed the solution above before adding 400µL of cell suspension (0.5-2×10^5 per well in a 24-well plate) to it. 1.5µl of lipofectamin 3000 (Invitrogen) reagent was added with 50µl of Opti-MEM. After 6 hours of incubation at 37°C/5%CO_2, the complexes were removed and the cells were incubated with cytokine-free media for up to 48h after transfection. The mRNA expression levels of BMI-2, Trx, TOPOIIα and UHRF1 were detected by real-time fluorescence quantitative PCR. The protein expressions of BMI-2, Trx, TOPOIIα and UHRF1 were detected by Western blotting. We also performed SA-β-gal staining and CFU-Mix formation assay to observe aging manifestation.

Chromatin immunoprecipitation (ChIP)

The cells were fixed with formamide at a final concentration of 1% to cross-link the H3K4me3 or H3K27me3 with DNA. After the cells were broken by lysis solution, DNA was sonicated to a size of 250-1000 bp (input DNA). The DNA protein complex was precipitated with specific antibodies (H3K4me3 or H3K27me3), absorbed onto the proteinA agar, decrosslinking. The precipitated DNA fragment was stored at -20ºC for long time. (This DNA fragment was named ChIPed DNA). Fluorescent quantitative PCR was used to detect TOPOIIα and UHRF1 levels of ChIPed DNA.

Statistical analysis

The experimental data was expressed as a mean and standard deviation. Single factor analysis of variance and one-way ANOVA was performed using SPSS 18.0. The LSD or Tamhane test was used to compare differences between two groups. $p<0.05$ was considered statistically significant.

Results

1. Purification of HSPCs

CD117, also known as c-kit, stem cell factor receptor. It is expressed on the majority of hematopoietic progenitor cells, including multipotent hematopoietic stem cells , committed myeloid precursor cells, erythroid precursor cells, and lymphoid precursor cells. CD117 is also expressed on a few mature hematopoietic cells such as mast cells. So, CD117 MicroBeads(Miltenyi biotec, Order no:130-091-224) are developed for the isolation of hematopoietic stem/progenitor cells and a few mature hematopoietic cells. The Lineage Cell Depletion Kit(Miltenyi biotec, Order no:130-090-858) is a magnetic labeling system for the depletion of mature hematopoietic cells, such as T cells, B cells, monocytes/macrophages, granulocytes and erythrocytes and their committed precursors from bone marrow. So, after centrifugation and sorting of Lin-c-Kit+, the Lin-c-Kit+ cells of BMCs are considered to be HSPCs (hematopoietic stem cell/progenitor cell).

HSPC purity was determined by Flow Cytometry Analysis. The purity of Lin−Kit+ cells was 94.4%(Fig.1d), 98.46%(Fig.1e)(n=10). It indicated that the sorted HSPCs are highly purified and suitable for subsequent experiments.

2. The establishment of old HSPCs model

HSPCs isolated from 4-weeks-old mice were cultured with the modeling medium including Stemspan Stem Cell Media, 10 ng/ml IL-3,10 ng/ml IL-6, 30 ng/ml SCF for 8 days. At day8, Flow cytometry was used to determine the ratio of HSPCs (Lin−c-Kit+). The results showed that the percentage of Lin−c-Kit+ cells at day8 was 76.3% (Fig.1f). It suggested HSPCs still have a high proportion at day8 and enough for testing.

3. The identification of old HSPCs model

To identify the old HSPCs model, the following experiments were performed: SA-β-gal staining, cell cycle distribution detection, colony forming assay, transmission electron microscope (TEM) and RNA-seq bioinformatics analysis. We further identify it by the comparative study on HSPCs isolated from old mouse(18-months-old) and old model HSPCs.

3.1 The percentage of SA-β-gal stain-positive cells increased

SA-β-gal (Senescence-associated-β-galactosidase) is a hallmark of aging that can yield a blue stain in the cytoplasm of aging cells[21-22]. We found that the percentage of SA-β-gal stain-positive cells increased gradually at day2, 4, 6, 8 compared with the young group (Supplementary Fig.S1). Therefore, the day8 was chosen as the optimum time of modeling. The percentage of SA-β-gal stain-positive cells in model group (day8) and in old mouse group were significantly higher than young group (day0) (Fig.2a, Table.1), $P<0.01$,$P<0.05$. The percentage of SA-β-gal stain-positive in model group (day8) was significantly higher than old mouse group (Table.1), $P<0.01$. (Fig. 2a). It indicated that the aging model group has more aging HSPCs than old mouse group.

3.2 The percentage of G0/G1 phase cells increased

Previous studies showed that senescent HSPCs were arrested in G0/G1[7, 18]. In the present study, we found that compared with the young group (41.93±1.95%), the proportion of G0/G1 phase cells in the model group was significantly higher (70.28±2.45%), $P<0.01$; the proportion of G0/G1 phase cells in old mouse group (46.59 ± 2.32%) was higher than the young group (41.93±1.95%), $P<0.05$, but the degree of increase was lower than the model group(Fig.2b, Table.2). The proportion of PI (S+G2/M) phase cells was significantly decreased in the model group compared with the young group, $P<0.05$ (Fig. 2b, Table. 2). These result showed that the aging model HSPCs were arrested in G0/G1.

3.3 Colony-forming ability decreased

The capacity to form CFU-mix decreased in HSPCs aging process[7, 18]. In our study, young group HSPCs formed CFU-E, CFU-G, CFU-M, CFU-GM and CFU-GEMM, whereas the model group HSPCs only occasionally formed CFU-G(Fig.2c). Furthermore, p-iodonitro- tetrazolium violet staining of CFU-mix experiment clearly showed that compared with the young group, model HSPCs displayed smaller and fewer colonies(Fig.2c). The number of CFU-Mix colonies formed by old mouse HSPCs was also reduced than that of the young group, but the degree of reduction was lower than that of the model group. These results revealed that the capacity of colony formation of the model HSPCs decreases significantly .

3.4 The ultrastructureof HSPCs changed

In order to visualize age-related ultrastructure changes of HSPCs, we explored it by using TEM method. It showed that the nuclear membrane of young HSPC was smooth and flat; there was homogeneous chromatin distribution and no or few inclusion body in cytoplasm (Fig. 2d). However, the perinuclear cisternae of model HSPCs widened, and the chromatin edge aggregated. A large number of inclusion bodies appeared in the model HSPCs. The presence of inclusion body may be due to aging of organelles that occurs when biomicromolecules are stored but not digested in the lysozyme, eventually accumulating in the cells to become brown liposarcoma[23-24]. Old mouse HSPCs show similar but less morphologic changes than aging model HSPCs(Fig.2d and Supplementary Fig.S2).

3.5 Age-related metabolic pathways changed by iTRAQ analysis

In order to study the changes of age-related metabolic pathways, we performed Quantitative proteomic analysis based on isobaric tags for relative and absolute quantitation (iTRAQ). The volcano plot(a) and the heat map(b) was shown in Fig3. Gene Ontology(GO) analysis revealed that the aging process increased significantly in model HSPCs compared with young group(p<0.01; Fig.3c). GO and KEGG(Kyoto Encyclopedia of Genes and Genomes) analysis consistently showed that the most differentially expressed proteins between the model group and the young group were associated with glycolysis, lysosomal, ribosomal synthesis and mRNA splicing (p<0.01; Fig.3c, Fig.3d). Glycolysis and lysosomal metabolism were significantly increased whereas ribosomal synthesis and mRNA splicing were significantly reduced in the model group compared with the young group(Table.3). Glycolytic metabolism increased in model vs young was consistent with the result of increased glycolysis metabolism in aging process shown by the previous study [25]. Lysosomal phagocytosis enhanced in model vs young was consistent with the electron microscopy data (Fig.2d). It may be due to a large number of damaged or aging cells and their metabolites, which are phagocytosed by lysosomes. The data also showed that mRNA splicing related proteins SR, hnRNP, WBP11, splicing factor 3b and U2AF1 were significantly decreased in model vs young (Table.3). It indicated that expression of spliced mRNA was significantly decreased. This conclusion is in line with recent research, which found that SF3B1, U2AF1 mutations led to an imbalance of hematopoietic function [26-27]. The results manifested that many aging related metabolic pathways changed in model vs young. In addition, STRING of iTRAQ showed that the common target proteins of PcG family and TrxG family are UHRF1 and TOPO IIα, as shown in Fig.3e. We validated it later in the paper.

3.6 Transcriptome changes by RNA-seq analysis

To identify transcriptome changes in the model group, we examined the expression of more than 16800 genes using RNA-seq. This analysis revealed 3717 genes that were up-regulated and 3931 genes that were down-regulated in model group vs young group, which is summarized as a scatter plot (Fig. 3f). As shown in (Fig.3g), the biological process of GO terms associated with the differentially expressed genes were related to aging and lysosomal metabolism, ribosomal synthesis and mRNA splicing. The result was consistent with our proteomics analysis. When applied to the Up- with-Age gene list, the analysis revealed a large number of enriched categories that have been linked to aging in general, such as NO-mediated signal transduction, the stress response (protein folding) and the inflammatory response, whereas categories enriched for Down-with-Age genes often included those involved in the preservation of genomic integrity, such as chromatin remodeling and DNA repair(Fig.3f). The result was consistent with Margaret A. Goodell's study[28]. A small hand-picked list is shown in Table 4, showed the most significant differences genes in the model group and the young group , consistent with the data of Margaret A. Goodell[28].

4. The factor of driving the model HSPCs aging

To explore what is the main factor of driving the model HSPCs aging we treated the cells with IL3(10ng/ml), IL6(10ng/ml), SCF(30ng/ml), media(no IL3, IL6, SCF), respectively or together with each other. We evaluate the aging effects with SA-β-gal staining and CFU-Mix method. The results showed a significant decrease in colony-forming ability and increase in SA-β-gal activity at IL3 groups compared with the control(medium) group(Fig.4 a,i,j). The cells cultured with IL3 alone or together with IL3 were mainly SA-β-gal positive and showed a significant decrease in the capacity of colony formation (Fig.4 a,b,c,d,i,j).There was no significant change in colony-forming ability and SA-β-gal activity at the cells cultured with IL6,SCF alone or together with IL6,SCF compared with the control(medium) group(Fig. 4 e,f,g,h,i,j).The previous study reported that the growth of HSC in vitro is strictly dependent on growth factors, in particular IL3[29].Zambrano A demonstrate that IL-3 contributes to cell survival under oxidative stress, a prominent feature in the aging process[30].In our study, contrary to these researches that IL3 is a positive factor of HSC growth in vitro or anti-aging of cells, our study showed IL3 can lead HSPC to senescence. However, our study was consistent with Catherine Frelin's study that showed Grb2 was positioned as a key adaptor integrating various cytokines response in cycling HSPC by IL3 signaling pathway[31]. Base on the previous researches and our study, we speculated the important roles of IL3 in activating HSPC senescence.

5.Polycomb/Trithorax system disturbance in HSPC aging process

To understand how cellular memory regulates HSPC aging, we examined the gene expressions of PCG(EZH1,BMI-2, EED,Rae-28, Mel18) and TrxG(MLL and Trx) with Realtime-PCR and Western blot. Furthermore, we explored target genes of PcG/TrxG sysytem and identified two genes, UHRF1/TOPOIIa.

5.1 The changes of Polycomb/Trithorax genes mRNA expression

The A260/280 ratio of RNA extracted from the HSPCs was 1.8-1.9, indicating high purity of RNA. The mRNA levels of EZH1, BMI-2 and EED, MLL in the model group were significantly lower than the young group, $p<0.01$ (Fig,5a,b,c,d) ;There are no significant differences in the mRNA levels of Mel18, Rae-28, Trx(Fig.5e,f,g).

5.2 The changes of Polycomb/Trithorax genes protein expression

The protein levels of EZH1, BMI-2,EED,Trx in model HSPCs were significantly lower than young HSPCs, (Fig.5h). MLL was significantly increased in the model group, $p<0.05$, (Fig.5h).The protein expressions of Mel18, Rae-28 were not significantly different in two groups,(Fig.5h). The data of STRING of iTRAQ might also provide us target genes of Polycomb/Trithorax, UHRF1 and TOPOIIα(Fig.3e). The protein levels of UHRF1 and TOPOIIα were significantly lower than young HSPCs, $p<0.05$. (Fig.5h).

To further explore the possible histone methylation regulation of Polycomb/Trithorax on the target genes, the levels of H3K4me3(trimethylation of histone H3K4) and H3K27me3 (trimethylation of histoneH3K27) were examined. H3K4me3 was known to be involved in gene transcriptional activation which can be

catalyzed by TrxG[32-33], and H3K27me3 is involved in transcriptional repression which can be catalyzed by PcG[34-35]. The total level of H3K27me3 or H3K4me3 was all significantly down-regulated in the model group compared with the young group(p<0.01) (Fig.5l,5j). The gray scale of Western Blot showed that the ratio of H3k4me3 /H3k27me3 in the young group was 0.6, whereas in the model group was 0.36 (Fig.5i,k). It is not difficult to find the reduction of H3K4me3 plays a leading role in HSPC aging process. So, whether TOPOIIα /UHRF1, which was significantly down-regulated, was regulated by the the general reduction of H3K4,or by a single factor, the reduction of H3K27me3 or H3K4me3 need to be further elucidated below in our study.

6. H3K4me3 of TOPOIIα and UHRF1 promoter decreased in model HSPC

To further validate H3K27me3/H3K4me3 of Polycomb/Trithorax on TOPOIIα/UHRF1, we examined it with CHIP-PCR. The data showed that the level of H3K4me3 in TOPOIIα or UHRF1 promoter was both decreased significantly in the model group (Fig.6a,b), but there was no significant change in the level of H3K27me3 in TOPOIIα or UHRF1(Fig.6c,d). Therefore, we speculated that H3K4me3, not H3K27, down-regulated TOPOIIα/UHRF1.

7. Knocking down Bmi-2/Trx down-regulated TOPOIIα/UHRF1 expression

To further validate TOPOIIα/UHRF1 was the target gene of PCG/TrxG, we studied the effect of knocking down Bmi-2 in PCG or Trx in TrxG on aging-related manifestations and the gene expressions of TOPOIIα and UHRF1. The results showed that the mRNA level and protein level of Bmi-2 or Trx was both significantly decreased after being transfected with Bmi-2 or Trx-siRNA for 48 h, respectively (p<0.05) (Fig.7a, b, c, d.), indicating that siRNA effectively knocked down Bmi-2 or Trx in HSPCs. The mRNA levels of TOPO2a and UHRF1 were both significantly decreased when Bmi-2 or Trx was knocked down, as shown in Fig.6e,f, p<0.05. SA-β-gal stained cells increased in Bmi-2 or Trx knocked down group, but there was not significantly difference(Fig.7g,h and Supplementary Table.S1), we speculated that cell aging caused by stress need enough time; colony-forming ability of HSPCs significantly decreased in Bmi-2 or Trx knocked down group compared with the control group, P<0.05, (Fig. 5 i,j). The results not only demonstrated TOPOIIα and UHRF1 were the target genes of Bmi-2 or Trx in HSPCs, but also indicated Bmi-2 and Trx were important members of PCG/TrxG. The loss of Bmi-2 or Trx caused the senescence of HSPCs that was probably mediated by TOPOIIα and UHRF1.

Discussion

Senescence HSPCs model in vitro is an important platform to study HSPC senescence and screen the anti-aging drug for hemopathy. Our study presented a quick and easy method of building senescence

HSPCs model *in vitro with* 4-week mouse. The method had the advantages including shorter time requirements, easyoperation.

Our senescence HSPCs model showed a significant increase in senescence-related β-gal activity, cell cycle arrest, reduction in colony-forming ability of HSPCs, age related changes in cell morphology and age related metabolic pathway. Furthermore, the model HSPCs showed more obvious aging manifestation compared with the HSPCs of natural aging mouse, so we speculated that this was a model of accelerating HSPCs aging in vitro compared with in vivo.

Polycomb group(PcG) and Trithorax group(TrxG) are evolutionarily conserved chromatin- modifying factors identified as histone methyltransferase complexes,which can methylate histone lysine-specific sites of target proteins. TrxG/PcG system maintain the balance of cellular memory system that prevents the change of stem cells identity by antagonizing each other[36-37]. In addition, in recent years they were found to have more widely control a plethora of cellular processes. This functional diversity is achieved by their ability to regulate chromatin at multiple levels, ranging from modifying local chromatin structure to orchestrating the three-dimensional organization of the genome.So,understanding TrxG/PcG system is a fascinating challenge of critical relevance for biology and medicine[38]. PcG proteins assemble in multimeric complexes, PRC1 and PRC2(Polycomb repressive complexes 1 and 2), and induce transcriptional repression of target genes through chromatin modifications such as H3K27me3[39-40]. Conversely, TrxG complex induce transcriptional activation of target genes through chromatin modifications such as H3K4me3[41]. PRC1 consists of ph1/Rae-28, Bmi-1, Mel-18 and other proteins in mammals[42] . The primary function of PRC1 is to label mono-ubiquitination of the 119th lysine site of histone H2A, thereby recruit PRC2 complex. PRC2 consists of EeD, Ezh2, Su(z)12 and other proteins, induce transcriptional suppression of target genes through chromatin modifications such as H3K27me3 and lysine26 on histone 1 (H1K26 me3)[43]. TrxG is mainly composed of Trx, Ashl and MLL. The previous study indicated that TrxG and PcG proteins can co-occupy and modify chromatin. TrxG protein-deposited histone modifications such as methylation at H3K4 can block PRC2 action and can, hence, antagonize PcG and counteract gene repression[44].Our study showed that the levels of PcG (EZH1, BMI-2, EED) and TrxG (MLL, Trx) were significantly changed in aging HSPCs and the changes were accompanied by obvious aging manifestations. It meant that the balance of TrxG/PcG system in HSPC was destroyed in aging process, so HSPC could not remember their own mission to continue differentiating into mature blood cells, hence, caused the aging of HSPC.

Furthermore, Western blot with anti-mouse H3K27me3 McAb and H3K4me3 McAb showed that aging HSPCs had a significantly lower levels of H3K27me3 and H3K4me3 compared with young HSPCs. As Petruk S noted in his study: Genetically, mutations in trxG and PcG genes can antagonize each other's function, whereas mutations of genes within each group have synergistic effects[45]. In our study, most of PcG and TrxG proteins were down-regulated, thereby we speculated it suppressed the levels of H3K27me3(by PcG) and H3K4me3(by TrxG). The data also implied that the regulating effects of

PcG/TrxG on the target genes maybe mediated by H3K27me3(by PcG) and H3K4me3(by TrxG), need further validation in our study.

About the target genes of PcG/TrxG, Hox genes were reported more frequently. Our ITRAQ STRING data hinted that the common target genes for PcG and TrxG were UHRF1 and TOPOIIα, we did further validation with siRNA and Chip-PCR. UHRF1 (ubiquitin-like with PHD and ring finger domains 1), also known as 90 kDa inverted CCAAT box binding protein (ICBP90) or nuclear phosphoprotein 95 (NP95). UHRF1 controlled the self-renewal versus differentiation of HSCs by epigenetically regulating cell-division modes, suggesting that UHRF1 could affects HSPCs' fate [46]. Topoisomerase(TOPO) is an enzyme that can cut DNA at a particular point to unravels the DNA twist and relieves the DNA supercoil nature. It plays an essential role during DNA replication. TOPOII(topoisomerase II) catalyse a transient double-strand DNA break, which allows the passage of another DNA duplex through the break before the strands are resealed. There are two isoforms of mammalian TOPOII, TOPOIIα and TOPOIIβ. The study of hematopoietic toxicity suggested that the level of TOPOIIα was decreased in bone marrow mononuclear cells of hematotoxic mice, accompanied by reduced acetylation of histone H4 and histone H3 on TOPOIIα promoter[47]. The previous study also demonstrated that TOPOIIα represents the target enzyme for haematological anticancer drugs, including for leukaemias, lymphomas[48]. These studies hinted the important roles of TOPOIIα and UHRF1 in anti-damaged of HSC/HSPC. In the present study, the levels of TOPOIIα and UHRF1 were both significantly down-regulated in aging group. RNA interference on Trx in TrxG or Bmi-2 in PcG down-regulated the gene expressions of UHRF1 and TOPOIIα. Meanwhile, it inhibited the colony-forming ability of HSPC. The results not only further indicated TOPOIIα and UHRF1 were the target genes of Bmi-2 or Trx that was important PCG/TrxG proteins in HSPCs, but also supported the role of TOPOIIα/UHRF1 in anti-damaged of HSPC.

Based on our hypothesis that TOPOIIαand UHRF1 were the target genes of PCG/TrxG in the process of HSPCs aging, we need to know if UHRF1 and TOPOIIα were methylated by H3K4me3 or H3K27me3 that was down-regulated by TrxG/PCG. CHIP-PCR assay showed that the H3K4me3 levels of TOPOIIα and UHRF1 promoter were lower in aging HSPCs compared with young HSPCs, whereas there was no significant difference in the H3K27me3 levels of TOPOIIα/UHRF1. We speculated that it may contribute to the decreased expression of TOPOIIα/UHRF1 in aging HSPCs because of H3K4me3 positive regulation on target genes[42]. Petruk S noted in his study“no overall synergism or antagonism between the trxG and PcG proteins and, instead, only subsets of trxG proteins act synergistically”[49]. Consistent with his study, our findings demonstrated UHRF1/ TOPOIIαwas regulated by H3K4me3 of TrxG.

Conclusion

In conclusion, our work proposed a quick and easy method of building aging HSPCs *in vitro with* 4-week mice which can be used for experimental study of HSPC senescence, forecasted that can be used for preliminary screen drugs of hemopathy. On the basis of this model and our preceding work on naturally aged mice, we made the point that TrxG/PcG disequilibrium impared cellular memory of HSPC, so that

HSC/HSPC could not remember their own mission to continue differentiating into mature blood cells, then led finally to cause or aggravate the aging of HSPCs. Our studies further identified UHRF1/TOPOII as target genes of TrxG/PcG system in HSPC aging process. TrxG/PcG disequilibrium shown in this paper extended our understanding of the molecular mechanisms underlying HSPC senescence.

Declarations

Ethics approval and consent to participate

Not applicable.

Consent for publication

Not applicable.

Availability of data and material

All data needed to evaluate the conclusions in the paper are present in the paper and/or the materials cited herein. Additional data related to this paper may be requested from the authors.

Competing interests

The authors declare that they have no competing interests.

Funding

This research was sponsored by the National Natural Science Foundation of China(No. 82074274,No.81403279).

Authors' contributions

L.N.Z. supervised the entire study including experimental design and data analysis, wrote the manuscript. Y.P.D and L.W.F conducted the experiments. W.X.Z. analyzed the data. All authors interpreted the data and approved the final manuscript.

Acknowledgements

We thank J.F.G. and M.K.H for critically reading the manuscript. We also acknowledge the efforts of many researchers, including the consortium members, who generated the foundational knowledge that made the program possible.

References

1. Luis TC, Tremblay CS, Manz MG, et al.Inflammatory signals in HSPC development and homeostasis: Too much of a good thing? Exp Hematol, 2016,44(10):908-12.

2. Abkowitz JL, Catlin SN, McCallie MT, et al. Evidence that the number of hematopoietic stem cells per animal is conserved in mammals. Blood. 2002;100(7):2665-2667.

3. Geng S, Mu XY, Chen XB, Hou JY, Jia DY, Xu CY, Wang YP: Study on the Dynamic Biological Characteristics of Sca-1(+) Hematopoietic Stem and Progenitor Cell Senescence. Stem Cells Int,2015:954120.

4. Li J, Cai D, Yao X, Zhang Y, Chen L, Jing P, Wang L, Wang Y: Protective Effect of Ginsenoside Rg1 on Hematopoietic Stem/Progenitor Cells through Attenuating Oxidative Stress and the Wnt/beta-Catenin Signaling Pathway in a Mouse Model of d-Galactose-induced Aging. Int J Mol Sci 2016;17.

5. Liran I. Shlush. Age-related clonal hematopoiesis. Blood,2018,131:496-504

6. Lee J, Yoon SR, Choi I, Jung H. Causes and Mechanisms of Hematopoietic Stem Cell Aging.Int J Mol Sci. 2019,13;20(6).

7. de Haan G, Lazare SS. Aging of hematopoietic stem cells.Blood. 2018,131(5):479-487.

8. Rando TA. Stem cells, ageing and the quest for immortality. Nature. 2006;441:1080–1086.

9. Flores-Guzman P, Fernandez-Sanchez V, Mayani H: Concise review: ex vivo expansion of cord blood-derived hematopoietic stem and progenitor cells: basic principles, experimental approaches, and impact in regenerative medicine. Stem Cells Transl Med 2013;2:830-838.

10. Flach J, Bakker ST, Mohrin M, Conroy PC, Pietras EM, Reynaud D, Alvarez S, Diolaiti ME, Ugarte F, Forsberg EC, et al: Replication stress is a potent driver of functional decline in ageing haematopoietic stem cells. Nature 2014;512:198-202.

11. Meng A, Wang Y, Van Zant G, Zhou D: Ionizing radiation and busulfan induce premature senescence in murine bone marrow hematopoietic cells. Cancer Res 2003;63:5414-5419.

12. Shao L, Feng W, Li H, Gardner D, Luo Y, Wang Y, Liu L, Meng A, Sharpless NE, Zhou D: Total body irradiation causes long-term mouse BM injury via induction of HSC premature senescence in an Ink4a- and Arf-independent manner. Blood 2014;123:3105-3115.

13. Tang YL, Zhou Y, Wang YP, Wang JW, Ding JC: SIRT6/NF-kappaB signaling axis in ginsenoside Rg1-delayed hematopoietic stem/progenitor cell senescence. Int J Clin Exp Pathol 2015;8:5591-5596.

14. Kamminga LM, de Haan G. Cellular memory and hematopoietic stem cell aging.Stem Cells. 2006 May;24(5):1143-9

15. Brand M, Nakka K, Zhu J, Dilworth FJ. Polycomb/Trithorax Antagonism: Cellular Memory in Stem Cell Fate and Function. Cell Stem Cell. 2019 Apr 4;24(4):518-533.

16. Tagoh H, Melnik S, Lefevre P et al. Dynamic reorganization of chromatin structure and selective DNA demethylation prior to stable enhancer complex formation during differentiation of primary hematopoietic cells in vitro. Blood 2004;103:2950 –2955.

17. Burrill DR, Silver PA: Making cellular memories. Cell 2010;140:13-18.

18. Dong Y, Lian X, Xu Y, Hu H, Chang C, Zhang H, Zhang L: Hematopoietic stem/progenitor cell senescence is associated with altered expression profiles of cellular memory-involved gene. Biosci Rep 2018;38.

19. Ringrose L, Paro R: Epigenetic regulation of cellular memory by the Polycomb and Trithorax group proteins. Annu Rev Genet 2004;38:413-443.

20. Wei Y, Zeng B, Zhang H, Chen C, Wu Y, Wang N, Wu Y, Shen L: iTRAQ-Based Proteomics Analysis of Serum Proteins in Wistar Rats Treated with Sodium Fluoride: Insight into the Potential Mechanism and Candidate Biomarkers of Fluorosis. Int J Mol Sci 2016;17.

21. Baker DJ, Sedivy JM: Probing the depths of cellular senescence. J Cell Biol 2013;202:11-13.

22. Bassaneze V, Miyakawa AA, Krieger JE: Chemiluminescent detection of senescence-associated beta galactosidase. Methods Mol Biol 2013;965:157-163.

23. Merkel KH: [Structure and aging processes in human menisci surfaces. A combination electron optic study with the transmission and the scanning electron microscope]. Verh Dtsch Ges Pathol 1978;62:482.

24. Gong YX, Sun Y, Xiang XR: [Transmission electron microscopic observation on the liver and cerebral cortex in aging mice treated with sijunzi decoction]. Zhongguo Zhong Xi Yi Jie He Za Zhi 1995;15:359-361.

25. Cho SJ, Moon JS, Lee CM, Choi AM, Stout-Delgado HW: Glucose Transporter 1-Dependent Glycolysis Is Increased during Aging-Related Lung Fibrosis, and Phloretin Inhibits Lung Fibrosis. Am J Respir Cell Mol Biol 2017;56:521-531.

26. Obeng EA, Chappell RJ, Seiler M, Chen MC, Campagna DR, Schmidt PJ, Schneider RK, Lord AM, Wang L, Gambe RG, et al: Physiologic Expression of Sf3b1(K700E) Causes Impaired Erythropoiesis, Aberrant Splicing, and Sensitivity to Therapeutic Spliceosome Modulation. Cancer Cell 2016;30:404-417.

27. Inoue D, Bradley RK, Abdel-Wahab O: Spliceosomal gene mutations in myelodysplasia: molecular links to clonal abnormalities of hematopoiesis. Genes Dev 2016;30:989-1001.

28. Chambers SM, Shaw CA, Gatza C, Fisk CJ, Donehower LA, Goodell MA. Aging hematopoietic stem cells decline in function and exhibit epigenetic dysregulation.PLoS Biol. 2007 Aug;5(8):e201.

29. Le Bousse-Kerdiles MC, Smadja-joffe F, Fernandez-Delgado R, Jasmin C.Organization of haematopoietic stem cells and their relationship to mastocytopoiesis. Ann Inst Pasteur Immunol. 1986 Sep-Oct;137D(2):187-99.

30. López C, Zamorano P, Teuber S, Salas M, Otth C, Hidalgo MA, Concha I, Zambrano A.Interleukin-3 Prevents Cellular Death Induced by Oxidative Stress in HEK293 Cells.J Cell Biochem. 2017 Jun;118(6):1330-1340.

31. CatherineFrelin, YishaiOfran, JulieRuston, et al. Grb2 regulates the proliferation of hematopoietic stem and progenitors cells.Biochimica et Biophysica Acta (BBA) - Molecular Cell Research,Biochim Biophys Acta Mol Cell Res. 2017,1864(12):2449-2459.

32. Lee BB, Choi A, Kim JH, Jun Y, Woo H, Ha SD, Yoon CY, Hwang JT, Steinmetz L, Buratowski S, et al: Rpd3L HDAC links H3K4me3 to transcriptional repression memory. Nucleic Acids Res, 2018,46(16):8261-8274.

33. Benayoun BA, Pollina EA, Ucar D, Mahmoudi S, Karra K, Wong ED, Devarajan K, Daugherty AC, Kundaje AB, Mancini E, et al: H3K4me3 Breadth Is Linked to Cell Identity and Transcriptional Consistency. Cell 2015;163:1281-1286.

34. Fontcuberta-PiSunyer M, Cervantes S, Miquel E, Mora-Castilla S, Laurent LC, Raya A, Gomis R, Gasa R: Modulation of the endocrine transcriptional program by targeting histone modifiers of the H3K27me3 mark. Biochim Biophys Acta 2018;1861:473-480.

35. Vieira W, Sahin H, Wells K, McCusker C: Trimethylation of Histone 3 lysine 27 (H3K27me3) ChIP-PCR and transcriptional expression data of Ef1-alpha, cyp26A, HoxC10, HoxD10 and HoxD11 in the Xenopus XTC cell line. Data Brief 2017;15:970-974.

36. Beerman I, Rossi DJ: Epigenetic regulation of hematopoietic stem cell aging. Exp Cell Res 2014;329:192-199.

37. Buszczak M, Spradling AC: Searching chromatin for stem cell identity. Cell 2006;125:233-236.

38. Schuettengruber B, Bourbon HM, Di Croce L, Cavalli G. Genome Regulation by Polycomb and Trithorax: 70 Years and Counting.Cell. 2017,171(1):34-57

39. Radulovic V, de Haan G, Klauke K: Polycomb-group proteins in hematopoietic stem cell regulation and hematopoietic neoplasms. Leukemia 2013;27:523-533.

40. Schnerch A, Lee JB, Graham M, Guezguez B, Bhatia M: Human embryonic stem cell-derived hematopoietic cells maintain core epigenetic machinery of the polycomb group/Trithorax Group complexes distinctly from functional adult hematopoietic stem cells. Stem Cells Dev 2013;22:73-89.

41. Powis G, Mustacich D, Coon A: The role of the redox protein thioredoxin in cell growth and cancer. Free Radic Biol Med 2000;29:312-322.

42. Lund AH, van Lohuizen M: Polycomb complexes and silencing mechanisms. Curr Opin Cell Biol 2004;16:239-246.

43. Di Croce L, Helin K: Transcriptional regulation by Polycomb group proteins. Nat Struct Mol Biol 2013;20:1147-1155.

44. Geisler SJ, Paro R. Trithorax and Polycomb group-dependent regulation: a tale of opposing activities.Development. 2015 Sep 1;142(17):2876-87.

45. Petruk S, Smith ST, Sedkov Y, Mazo A. Association of trxG and PcG proteins with the bxd maintenance element depends on transcriptional activity. Development. 2008 Aug;135(14):2383-90

46. Zhao J, Chen X, Song G, Zhang J, Liu H, Liu X: Uhrf1 controls the self-renewal versus differentiation of hematopoietic stem cells by epigenetically regulating the cell-division modes. Proc Natl Acad Sci U S A 2017;114:E142-E151.

47. Shi Y, Qian S, Li J, Yu K: [Histone acetylation modification of topoisomerase enzyme alpha promoter regulation factors in patients with chronic benzene poisoning]. Zhonghua Lao Dong Wei Sheng Zhi Ye Bing Za Zhi 2016;34:8-12.

48. Rossi E, Villanacci V, Bassotti G, et al. TOPOII alpha and HER-2/neu overexpression/ amplification in Barrett's oesophagus, dysplasia and adenocarcinoma. Histopathology. 2010,57(1):81-9

49. Petruk S, Smith ST, Sedkov Y, Mazo A. Association of trxG and PcG proteins with the bxd maintenance element depends on transcriptional activity.Development. 2008 Aug;135(14):2383-90.

Tables

Table 1 Percentage of SA-β-gal stain-positive HSPCs (% x ± s, n=10)

Group	%
Young group	1.02±0.09
Model group	56.4±5.21**
Old mouse group	7.16±1.14*

* P0.05, compared with the young group;**P0.01, compared with the young group.

Table 2 Distribution of cell cycles of HSPCs (x±s,n=5)

Group	G0/G1	G2/M	S
Young group	41.93±1.95	12.38±0.20	45.69±2.06
Model group	70.28±2.45*	7.28±0.39*	22.45±1.57*
Old mouse group	46.59±2.32	12.64±0.69	40.77±2.15

* P□0.05, compared with the young group.

Table3 Differently expressed genes in the KEGG metabolic pathway (Model group/Young group)

Accession	Description	Gene name	Fold change ratio
G3UVV4	Hexokinase 1	Hk1	1.2
Q3TRM8	Hexokinase-3	Hk3	1.57
P12382	ATP-dependent 6-phosphofructokinase	Pfkl	0.88
Q9WUA3	ATP-dependent 6-phosphofructokinase platelet type	Pfkp	1.66
P52480	pyruvate kinase	Pkm	1.96
P35486	Pyruvate dehydrogenase E1 component subunit alpha	Pdha1	0.95
O70370	Cathepsin S	Ctss	1.87
O89023	Tripeptidyl-peptidase 1	TPP1	1.71
O35114	Lysosome membrane protein 2	Scarb2	1.82
P11438	Lysosome-associated membrane glycoprotein 1	Lamp 1	1.91
P17047	Lysosome-associated membrane glycoprotein 2	Lamp 2	1.42
P50516	V-type proton ATPase catalytic subunit A	Atp6v1a	1.94
Q9Z204	Heterogeneous nuclear ribonucleoproteins C1/C2	Hnrnpc	0.63
Q923D5	WW domain-binding protein 11	WBP11	0.6
Q921M3	Splicing factor 3b subunit 3	SF3B3	0.81
Q3UJB0	Splicing factor 3b subunit 2	SF3B2	0.62
Q9D883	Splicing factor	U2af1	0.5
Q9Z204	Heterogeneous nuclear ribonucleoproteins C1/C2	Hnrnpc	0.63

Table 4. Differently expressed genes Selected (Model group/ Young group)

Symbol	Gene Name	log_2FC	Significance
Xab2	XPA binding protein 2	-1.02	DNA repair
Sirt3	Sirtuin 3	-1.04	Chromatin silencing
Sirt	Sirtuin	-1.57	Chromatin silencing
Rad52	RAD52 homolog	-1.62	DNA repair
Xrcc3	X-ray repair comp. defective repair in C. hamster cells 3	-2.32	DNA repair
Eng	Endoglin	-2.81	TGF-b regulates HSPCs pool size
Blm	Bloom syndrome homolog	-1.48	DNA repair
Sirt	Sirtuin 2	-1.57	Chromatin silencing
App	Amyloid beta precursor protein	4	Alzheimer disease, stress response
Selp	Platelet-selectin	2.47	Inflammation, adhesion
Ctsb	Cathepsin B	3.56	APP processing, Alzheimer
Ctsc	Cathepsin C	4.85	Proteolysis, inflammation
Icam1	Intercellular adhesion 1	4.2	Cell-cell adhesion, inflammation
Ctss	Cathepsin S	7.4	Proteolysis, inflammation
Cct6a	Chaperonin subunit 6a (zeta)	1.34	Protein folding
Dnajb6	DnaJ (Hsp40) homolog B6	2.8	Protein folding
Tlr4	Toll-like receptor 4	2.08	Inflammation

Table.S1 Percentage of SA-β-Gal positive HSPCs (% x ± s, n=3)

Group	%
Negative control	2.71±0.03
siRNA Trx	7.62±0.47
siRNA Bmi-1	7.50±0.32

* P□0.05, compared with Negative control

Figures

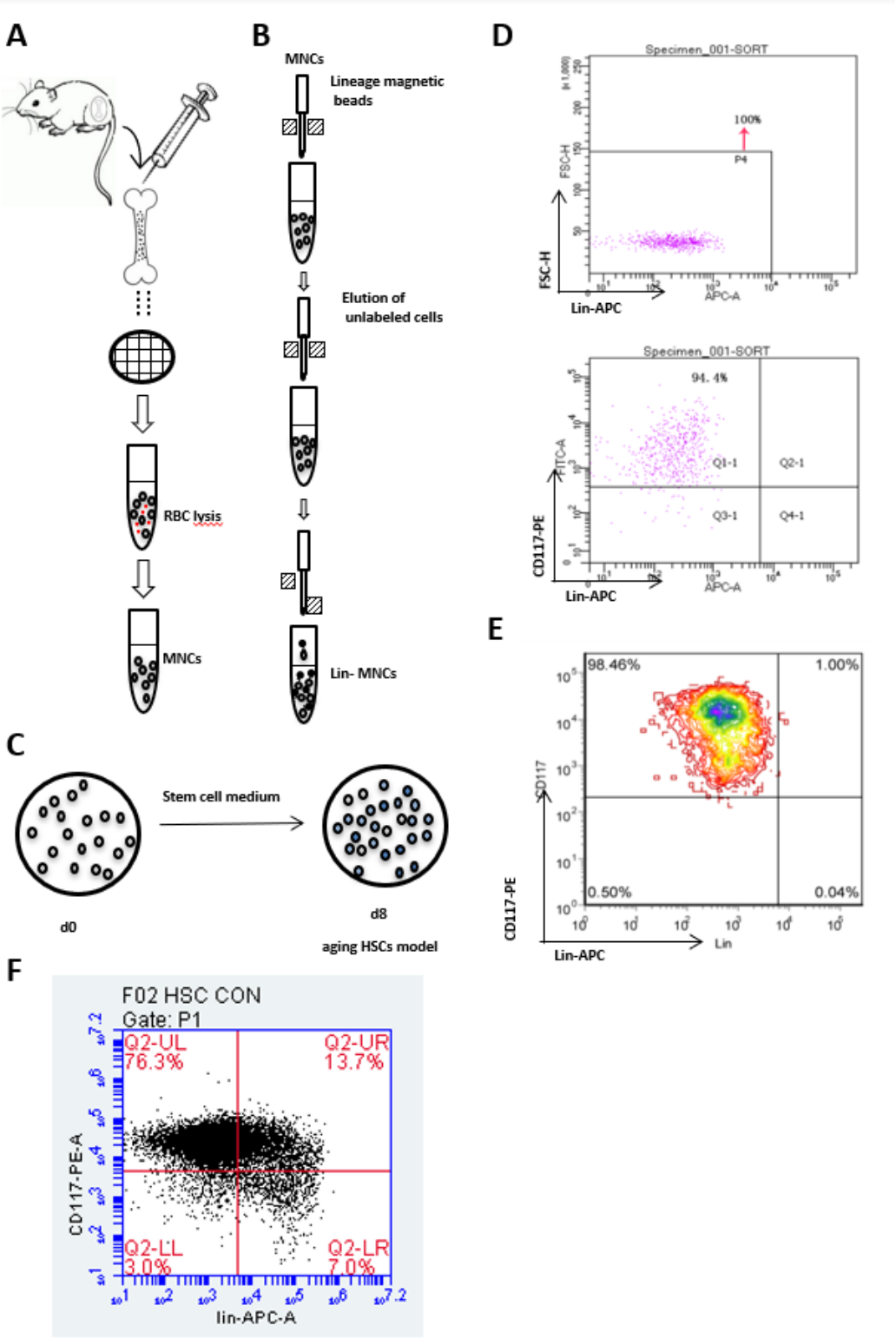

Figure 1

HSPCs were effectively isolated and purified by MACS (a). Schematic illustrates the isolation of mouse bone marrow mononuclear cells (MNCs). (b). For lineage depletion, cells were magnetically labeled with a cocktail of biotinylated antibodies that are against a panel of so-called “lineage” antigens (CD5, CD45R

(B220), CD11b, anti-Gr-1 and Ter-119 antibodies) and anti-Biotin MicroBeads. This labeling procedure leaves the lineage negative cells undisturbed, thus allowing further separation of lineage– cells. Then the lineage– cells (lin- cells)were purified by c-Kit MACS, namely lin-c-Kit+ cells. (c). HSPCs were cultured with specific modeling medium (stem cell culture medium + 10 ng/ml IL3 + 10 ng/ml IL6 + 30ng/ml SCF) and incubated for 8 days, it's model group. (d,e). Flow cytometric analysis of the purity of lin–c-Kit+ cells at day0. (f). Flow cytometric analysis of the purity of lin–c-Kit+ cells at day8. The results were expressed as mean ± S.D. and the p values (*P < 0.05, **P < 0.01, ***P < 0.001) were determined by Anova test.

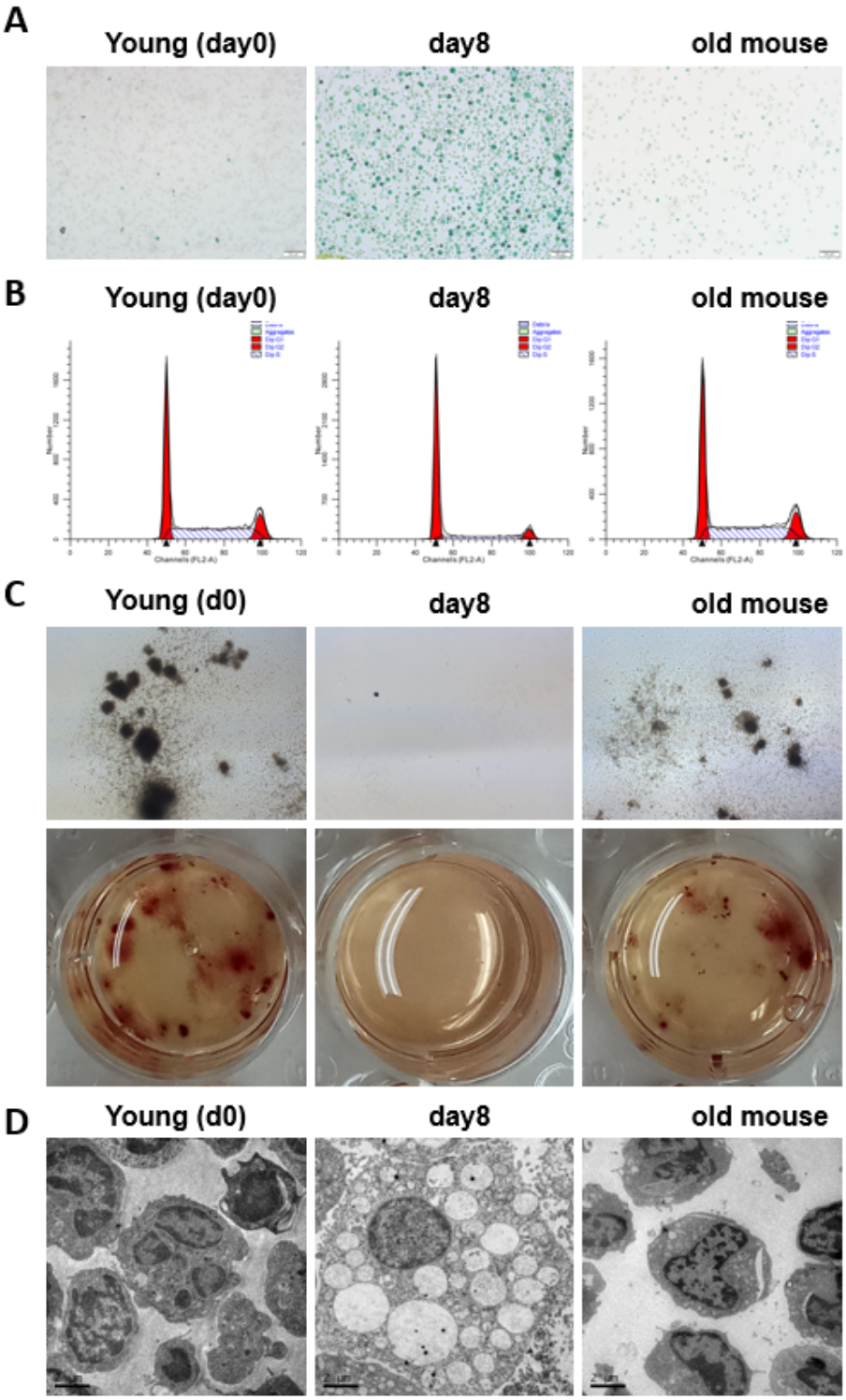

Figure 2

Model HSPCs showed significant manifestations of aging such as increased β-galactosidase activity, G0/G1 phase arrest, decreased colony forming capacity and changes in cell morphology. (a). Photomicrographs of SA-β-gal staining(×200). The percentage of SA-β-gal stain-positive cells was significantly increased in the model group compared with the young group, n=10. (b). Flow-cytometric analysis of cell cycle distribution. The model HSPCs were arrested in G0/G1 phase compared with the young group, n=10. (c). Photomicrographs of CFU-Mix. The size and number of CFU-Mix significantly decreased in the model group compared with young group. (d). Photomicrographs of TEM. The nuclear membranes of young HSPCs was smooth and flat, chromatin evenly distributed; there were few to no inclusion bodies found in the cytoplasm . But the perinuclear cisternae in the model HSPCs widened, and chromatin edge aggregated. A large number of inclusion bodies appeared in the model HSPCs.

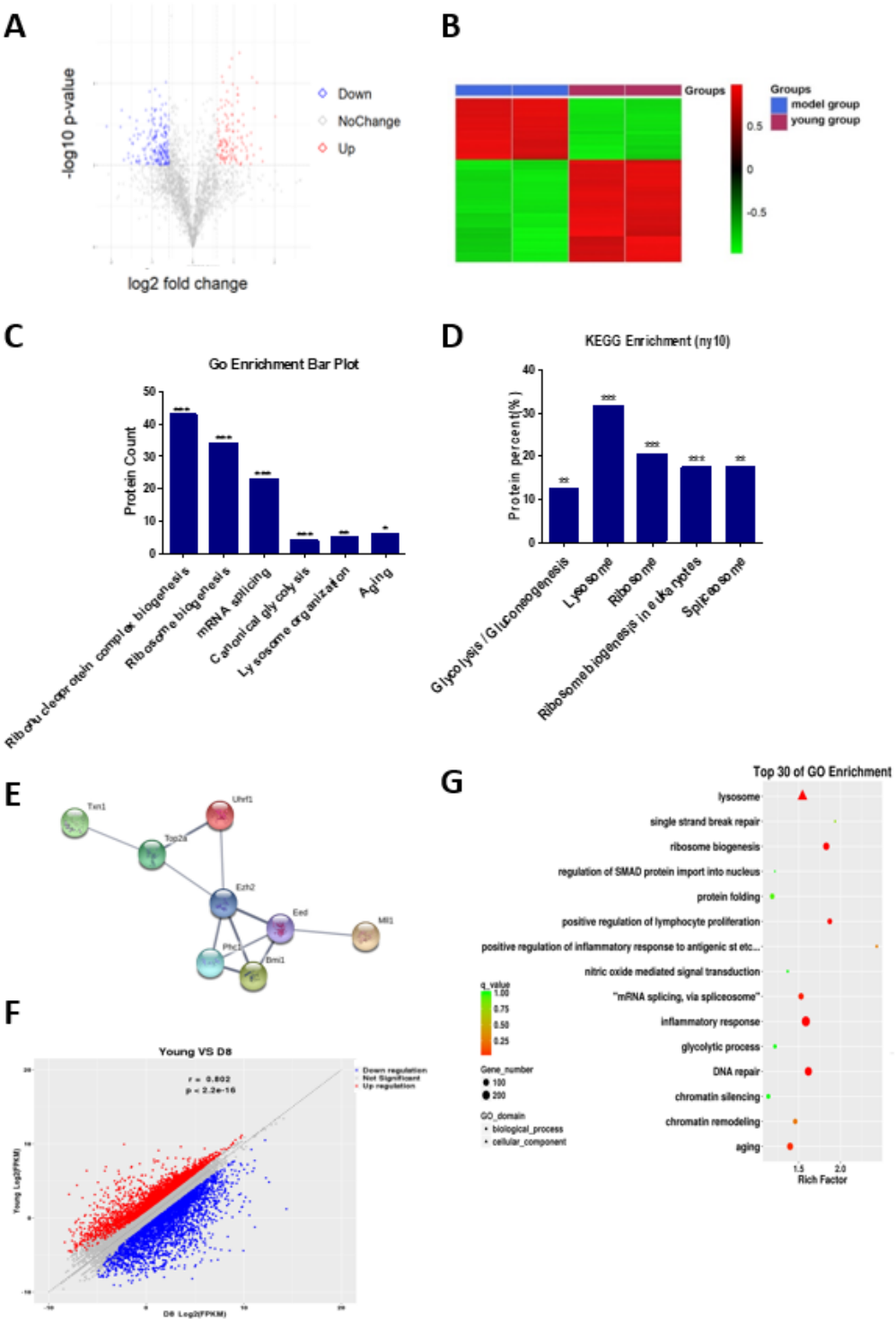

Figure 3

Integrated Proteomic and Transcriptomic Analysis showed significant changes of metabolic processes associated with aging in Model HSPCs. (a). The volcano plot of proteomic, which plots significance versus fold-change on the y and x axes respectively, finded up-regulated and down-regulated proteins using t-test. Red color represents the up-regulated proteins and blue color represents down-regulated proteins. (b).The heat map of proteomic, showed protein expression levels of the young group and the

model group. Color intensity indicates level of expression, where green signifies low expression and red signifies high expression. (c).Gene Ontology analysis of proteomics , p<0.05. (d). KEGG analysis of proteomics. Go enrichment (c) and KEGG pathway (d) analysis showed that glycolysis, lysosomal metabolism, ribosomal synthesis and mRNA splicing were significantly changed in the model. (e). STRING analysis of proteomics showed that the common target proteins of PcG and TrxG are UHRF1 and TOPOIIa. (f). The scatter plot of transcriptomic, red dots were up- regulated and blue dot were down-regulated. (g).Go enrichment analysis of transcriptomic, showed genes associated with the stress response, inflammation, lysosomal metabolism and protein aggregation dominated the up-regulated expression profile, while the down-regulated profile was marked by genes involved in the preservation of genomic integrity and chromatin remodeling.

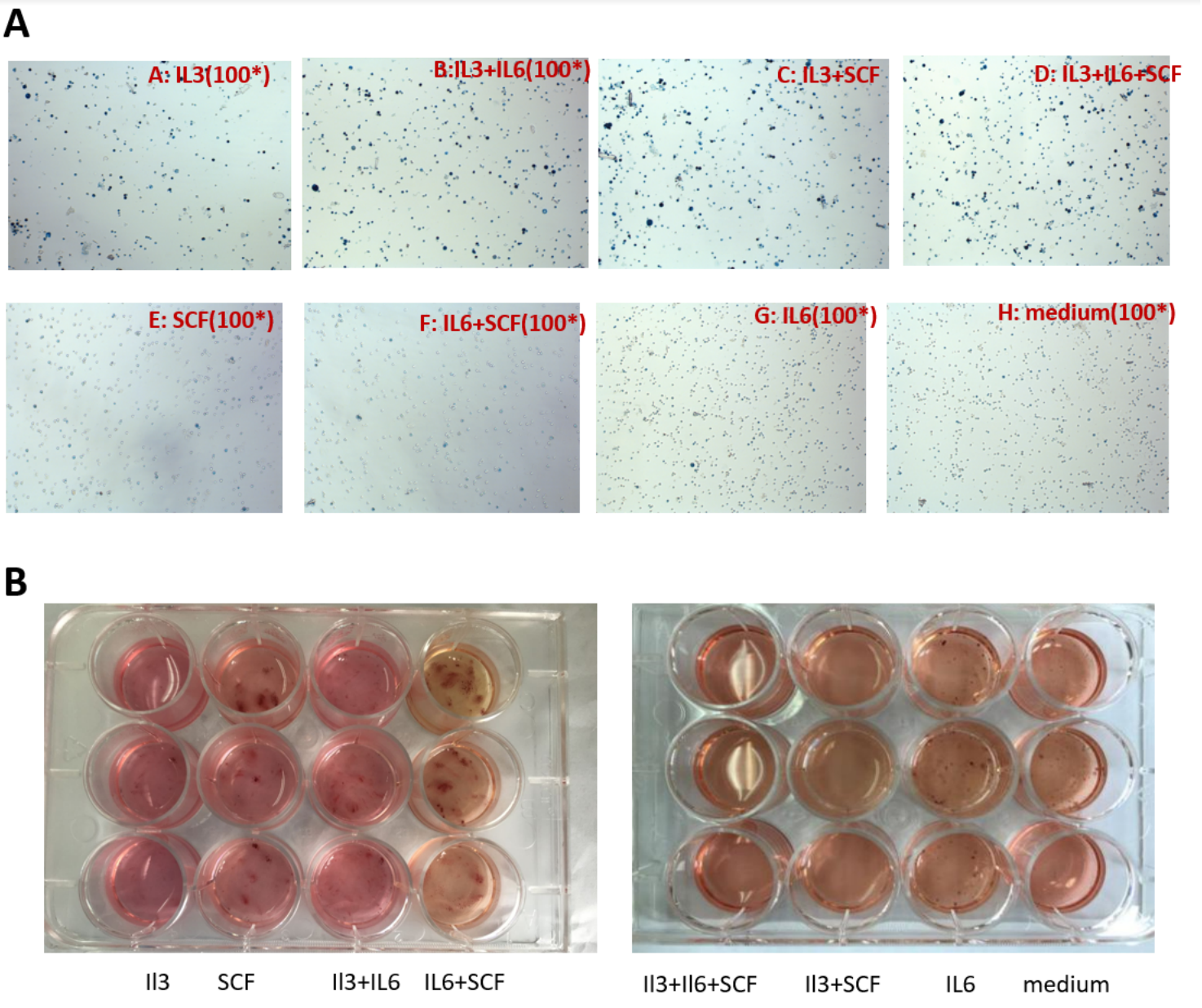

Figure 4

The factor of driving the model HSPCs aging (a,b,c,d,e,f,g,h). Photomicrographs of SA-β-gal staining(×100). The cells cultured with IL3 alone or together with IL3 were mainly SA-β-gal positive. There was no significant change in SA-β-gal activity at IL6,SCF alone group or together with IL6,SCF group. (i,j). Photomicrographs of CFU-Mix. The cells cultured with IL3 alone or together with IL3 showed a significant decrease in colony-forming ability.There was no significant change in colony-forming ability at IL6,SCF alone group or together with IL6,SCF group.

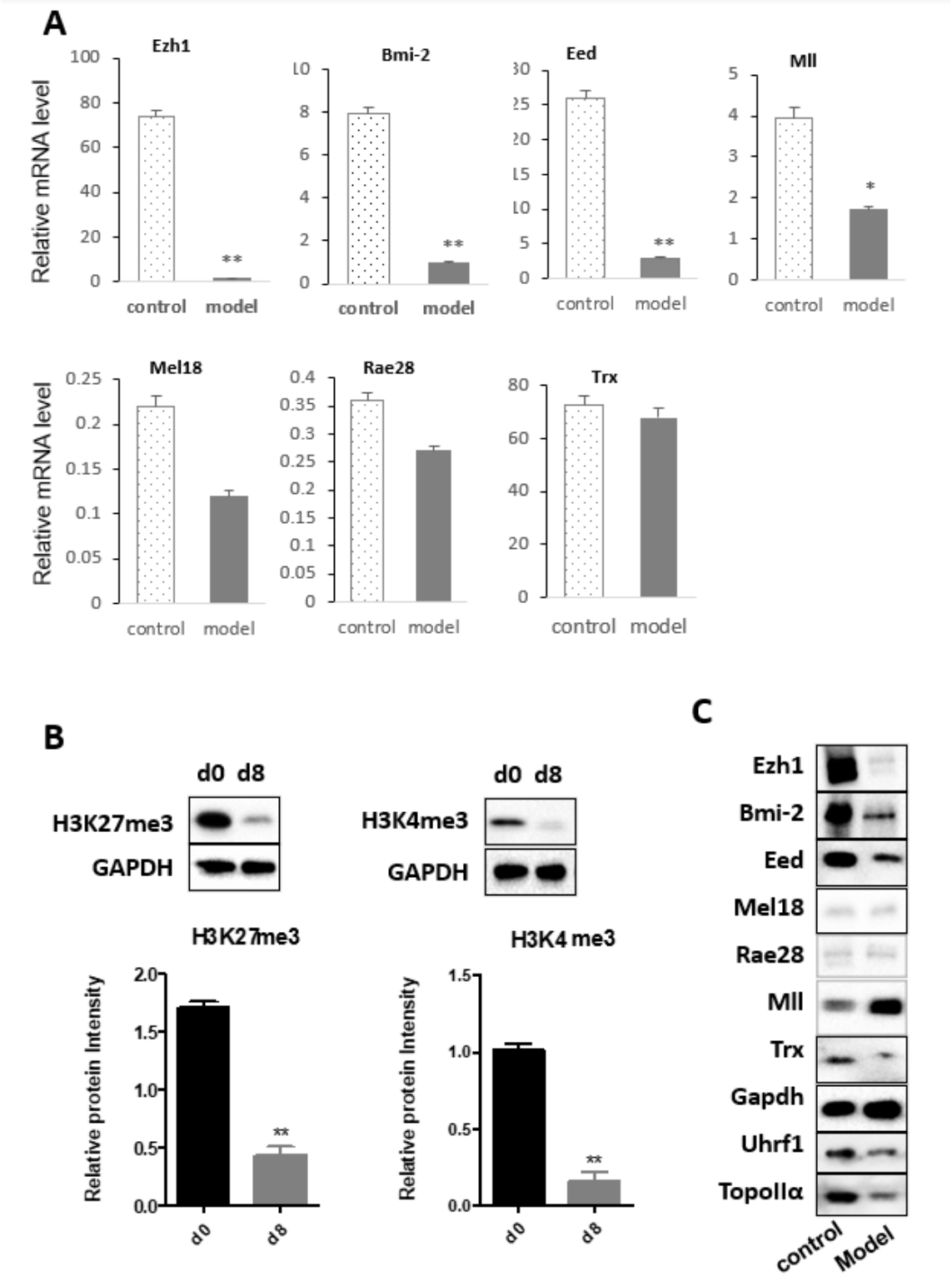

Figure 5

Polycomb/Trithorax system disturbance in HSPC aging process RT-PCR was applied to determine the transcription levels of PcG/TrxG genes(a,b,c,d,r,f,g). Western Blot was applied to determine the levels of PcG/TrxG proteins(h) and H3K4 (i,j),H3K27 (k,l),TOP2a (h),URHF1 (h).

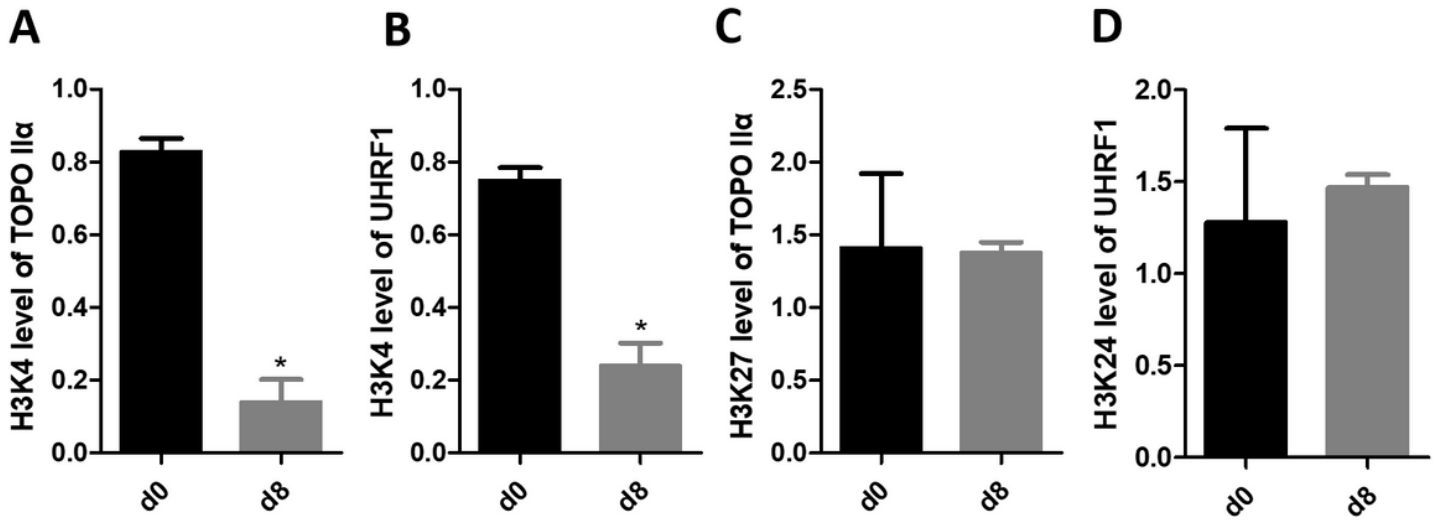

Figure 6

CHIP-PCR showed H3K4me3 of TOPOIIα and UHRF1 promoter decreased in senescent HSPCs.(a,b). The level of H3K4me3 in TOPOIIα/UHRF1 promoter was decreased in aging HSPCs.(c,d). There was no significant change in the level of H3K27me3 in TOPOIIα/UHRF1 promoter in aging HSPCs.

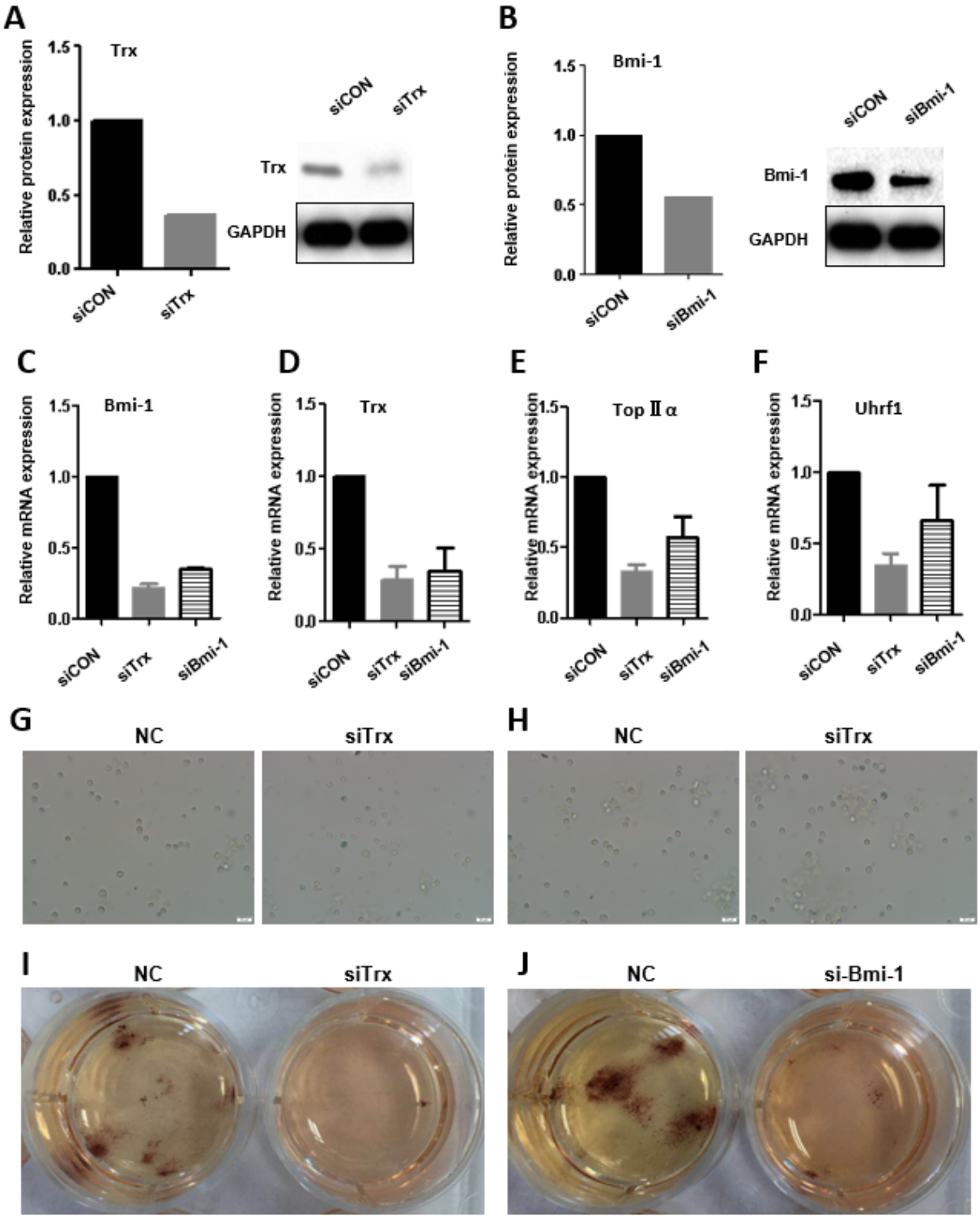

Figure 7

Bmi-1 and Trx were important members of PCG/TrxG protein and Knocking down Bmi-2/Trx down-regulated TOPOIIα/UHRF1 expression. (a,b). HSPCs from 4- weeks-old mice were transfected with Bmi-1-siRNA and Trx-siRNA at 48 h. Bmi-1 gene expression (b,c) and Trx gene expression (a,d) were validated by Realtime-PCR and WB analysis. mRNA expression of TOPO□α (e), UHRF1(f) decreased significantly in Bmi-1 or Trx knocked down group. SA-β-gal stained cells increased in Bmi-2 or Trx knocked down

group,but there was not significantly difference(h). colony-forming ability of HSPCs significantly decreased in Bmi-1(j) or Trx(i) knocked down group compared with the control group.

Supplementary Files

This is a list of supplementary files associated with this preprint. Click to download.

- S1.png
- S2.png
- S3.png